



New insights on physico-chemical investigation of bisphosphonate adsorption isotherm into apatite substrate using statistical physics treatment

Aljawhara H. Almuqrin^a, Sarra Wjihi^{b,*}, Fatma Aouaini^{a,b}, Abdelmottaleb Ben Lamine^b

^a Physics Department, Faculty of Science, Princess Nourah Bint Abdulrahman University, Riyadh, Saudi Arabia

^b Laboratory of Quantum and Statistical Physics, LR18ES18, Faculty of Sciences of Monastir, Tunisia

ARTICLE INFO

Article history:

Received 25 February 2020

Received in revised form 18 April 2020

Accepted 23 April 2020

Available online 26 April 2020

Keywords:

Adsorption isotherm

Statistical physics model

Osteoporosis disease

Thermodynamics function

ABSTRACT

In this paper, a well-crystallized hydroxyapatite (HA) and nanocrystalline apatites (NCA) were used to interpret the adsorption process of two bisphosphonates (BPs), namely Tiludronate (Tilu) and Risedronate (Rise). These BPs are among the most prescribed classes of drugs for the treatment of bone disorders disease, particularly Osteoporosis. The equilibrium data used to express the variation of uptake capacity as a function of concentration were determined by varying some experimental physicochemical conditions (e.g. temperature and pH). A preliminary analysis of all the adsorption isotherms obviously indicates that the adsorption quantity tends towards a saturation level. This suggests a finite number of adsorbed layers involved in the adsorption mechanisms. To give a reasonable analysis of the drug adsorption process, three advanced models are proposed and developed in the light of a statistical physics treatment which is tested and discussed. The modeling analysis reveals that the adsorption of the two drugs occurs by the formation of two different adsorbed layers on the apatite surface. Based on the analysis of the selected model parameters, it was deduced that both drugs molecules were anchored alternately with parallel and non-parallel positions on the apatite substrate. The study of the uptake capacities at saturation showed that these parameters followed the sequence: $Q_{\text{asat}}(\text{Rise-NCA}) > Q_{\text{asat}}(\text{Rise-HA}) > Q_{\text{asat}}(\text{Tilu-HA})$, indicating that the NCA adsorbent was more effective for the Rise drug adsorption than the HA adsorbent. The estimated adsorption energies globally varied from 9.20 to 19.52 kJ/mol, confirming the physical nature of the adsorption process for the investigated systems. Conventionally, to characterize the adsorption process, the entropy (S_a), the enthalpy of Gibbs (G) and the internal energy (E_{int}) were treated and interpreted.

© 2020 Elsevier B.V. All rights reserved.

1. Introduction

The bone tissue is composed of an organic phase consisting essentially of collagen and a mineral phase consisting of a nanocrystalline phosphocalcic apatite. These apatite nanocrystals have two major characteristics: a complex structure with a hydrated layer on the surface of the apatite core and an alteration of their composition with age modifying the constitution of the mineral phase. Bone tissue is constantly renewing and this “bone remodeling” results from the combined action of two types of cells: cells resorbing bone (osteoclasts) and cells that rebuild bone (osteoblasts). An imbalance in this renewal can appear in the case of frequent bone diseases like Osteoporosis. It is well-known as a silent disease because it evolves without symptoms. It is more common in women, especially after menopause caused by the decrease of the estrogen level. Bisphosphonates (BPs) are a promising class of drugs for

the treatment and prevention of this bone disorders disease. It has a strong affinity for adsorption on bone minerals and prevents the dissolution of minerals and bone resorption, thus inhibiting the Osteoclasts activity. BPs have two different functionalities in their chemical structure connected to the center of carbon. This leads to a significant improvement of both the mineral adsorption affinity and the cellular activity; the ability of BP molecules to link to bone mineral is increased by a functional group that binds to calcium like the hydroxyl group (OH) [1,2], and by groups having a nitrogen atom within a heterocyclic ring such as the risedronate and zoledronate molecules [3]. The classic treatment using BP drugs is performed by oral administration or intravenous injection. However, this systemic use of BPs can cause undesirable side effects such as ulcers [4,5], Osteonecrosis of the jaw, particularly by intravenous injection [6] and fever [7]. To avoid these undesirable effects and increase BPs bioavailability, it is very important to define strategies for local administration of such antiosteoporotic drugs at bone sites presenting a risk of fracture. Thus, many studies have been realized to explain the interactions between BP molecules and bone or calcium phosphate substrate for a deeper understanding of their adsorption

* Corresponding author at: Department of Physics, Faculty of Sciences of Monastir, Boulevard de l'Environnement, 5019 Monastir, Tunisia.

E-mail address: sarawjihi@yahoo.fr (S. Wjihi).

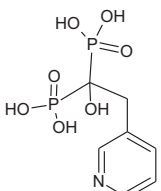
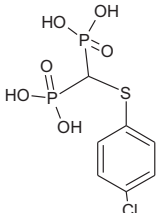
process [8–11]. In this work, the important and significant point is to reveal through the adsorption process modeling, all the physico-chemical properties of the Bisphosphonate drug adsorption to better understand the metabolism and the medicine work in organic cellular tissues of the human body. Many similar systems have been studied by applying empirical/semi-empirical models providing classical interpretations [12–16]. These interpretations have led to an incomplete understanding of the adsorption mechanism. Since all their parameters are mathematical, they have no physical meaning. None of the models of the literature [12–16] use our statistical approach, especially the particular parameters introduced in our models. The only concern of these studies is about the adsorption energies, which are most often deduced empirically, and sometimes about the number of types of sites which is qualitatively provided. This paper introduces an advanced statistical physics framework that simulates the adsorption of risedronate and tiludronate on two apatite substrates (NCA and HA). An assessment based physical model provides a new vision of the Bisphosphonate adsorption mechanism by investigating their physicochemical parameters, such as the number of attracted molecules per main adsorption site, density of receptor sites, and concentrations at half-saturation. For instance, the orientation of the adsorbate on the adsorbent surface is sketched in the paper for the first time at each adsorption temperature and pH. This description of the adsorbate orientation provides interesting ideas to further explain the BP adsorption mechanism. Interestingly, all the physical model parameters contribute to assign a new vision of the BP adsorption mechanism since they are characterized by a clear physical meaning unlike the empirical models.

2. Material and method

In this paper, the adsorption isotherms of risedronate (Rise) and tiludronate (Tilu) on well-crystallized hydroxyapatite (HA) and nano-crystalline apatites (NCA) were used. These adsorption equilibrium data were quantified in a previous work [17] which provides a complete demonstration of the adopted experimental methodologies. The adsorption experiments were performed under different physicochemical conditions to detect the influence of temperature (physiological temperature of 310 K and room temperature of 298 K) and pH (at levels 6.6, 7.4 and 9.5).

Some physical properties of both risedronate (Rise) and tiludronate (Tilu) are given in Table 1.

Table 1
Physical properties of risedronate and tiludronate.

Compound	Structure	Formula	Weight (g mol ⁻¹)	Solubility (mg/ml)
Risedronate		C ₇ H ₁₁ NO ₇ P ₂	283.11	10.4
Tiludronate		C ₇ H ₉ ClO ₆ P ₂ S	362.57	6.97

3. Modeling analysis

Three adsorption isotherm models were developed to adjust the experimental isotherm data. Therefore, the isothermal parameters obtained from these models were interpreted to understand the BP adsorption equilibrium on HA and NCA. Specifically, these models were established using the grand canonical ensemble in statistical physics. All of these models are succinctly illustrated in the following subsections.

3.1. Monolayer model with single energy (M1)

This statistical physics model suggests that the adsorption of Tilu and Rise occurs via the creation of a single layer with one adsorption energy for all receptor sites. Several approximations are considered. First, the mutual interactions between the adsorbate molecules are neglected because the work conditions are far from the solubility (C_s), as supposed in [18]. Second, the internal degrees of freedom of the Rise and Tilu molecule can be neglected, except the translational degree. This is because it is not possible to thermally excite the electronic degree of freedom. Moreover, the vibrational degree of freedom can be neglected compared to the translational degree [18,19].

To establish the model, the grand canonical ensemble in statistical physics is used. The grand canonical partition function of a single site is the following:

$$Z_{gc} = 1 + e^{\beta(\varepsilon_1 + \mu)} \quad (1)$$

where ($-\varepsilon_1$) is the adsorption energy of the receptor site, μ is the corresponding chemical potential and β is defined as $1/k_B T$, where k_B is the Boltzmann constant and T is the absolute temperature.

Then, the total grand canonical partition function related to the density of receptor sites D_{sr} , is assumed to be identical and independent. This function is expressed in Eq. (2).

$$Z_{gc} = \left(1 + e^{\beta(\varepsilon_1 + \mu)}\right)^{D_{sr}} \quad (2)$$

The average site occupation number is expressed as follows [18]:

$$N_0 = k_B T \frac{\partial \ln Z_{gc}}{\partial \mu} = N_M k_B T \frac{\partial \ln Z_{gc}}{\partial \mu} \quad (3)$$

This model also assumes that every receptor site (S) accepts a variable number of Tilu or Rise molecules following the adsorption reaction:



When the thermodynamic equilibrium is reached according to Eq. (4), the relation between the different chemical potentials may be expressed as: $\mu_m = \mu/n_{ms}$, where μ_m and μ are the chemical potential of dissolved molecules and the chemical potential of adsorbed molecules, respectively, and n_{ms} is the number of molecules per site. In addition, μ_m can be expressed as follows [19]:

$$\mu_m = k_B T \ln \frac{N}{Z_g} \quad (5)$$

where $Z_g = Z_{gtr}$ is the translation partition function which can be expressed as [18,19]:

$$Z_g = Z_{gtr} = V \left(\frac{2\pi m k_B T}{h^2} \right)^{3/2} \quad (6)$$

where V is the gas volume, m is the adsorbed molecule mass and h is the Planck constant.

Using Eq. (4) and the number of average site occupation N_o , the average number of adsorbed molecules is written as:

$$Q_a = n_{ms}N_o \tag{7}$$

The analytical expression of this model is given by [18]:

$$Q_a = \frac{n_{ms} \cdot D_{sr}}{\left(1 + \left(\frac{C}{C_{hs}}\right)^{n_{ms}}\right)} \tag{8}$$

where n_{ms} is the number of Tilu and Rise molecules per receptor site, D_{sr} is the density of receptor sites, C_{hs} is the concentration at half-saturation of Tilu and Rise adsorbed on HA and NCA.

Subsequently, this statistical theory is used in all models employed in this work.

3.2. Double layer model with two energies (M2)

For this model, we consider that the Tilu and Rise adsorption is achieved via the formation of two adsorbate layers involving two interaction energies. We can assume that the first adsorbed layer has an adsorption energy ($-\varepsilon_1$) and the second has a different adsorption energy ($-\varepsilon_2$) which should be lower than ($-\varepsilon_1$), because the first molecules are adsorbed directly on the surface and so they have a higher energy. The grand canonical partition function of one site is written as:

$$z_{gc} = 1 + e^{\beta(\varepsilon_1 + \mu)} + e^{\beta(\varepsilon_1 + \varepsilon_2 + 2\mu)} \tag{9}$$

The partition function related to D_{sr} receptor sites is written as:

$$Z_{gc} = \left(1 + e^{\beta(\varepsilon_1 + \mu)} + e^{\beta(\varepsilon_1 + \varepsilon_2 + 2\mu)}\right)^{D_{sr}} \tag{10}$$

According to the theory detailed in Section 3.1, the expression of the double-layer model with two energies can be written as follows [19]:

$$Q_a = n_{ms}D_{sr} \frac{\left(\frac{C}{C_{hs1}}\right)^{n_{ms}} + 2\left(\frac{C}{C_{hs2}}\right)^{2n_{ms}}}{1 + \left(\frac{C}{C_{hs1}}\right)^{n_{ms}} + \left(\frac{C}{C_{hs2}}\right)^{2n_{ms}}} \tag{11}$$

where C_{hs1} and C_{hs2} are the concentration at half-saturation of the first and second layers.

3.3. Multilayer model with saturation (M3)

This generalized statistical physics model assumes that the sorption of the Tilu and Rise molecules on the two tested adsorbents occurs via the creation of a variable number of layers with two different adsorption energies [20]. The first energy ($-\varepsilon_1$) can characterize the interactions between the Tilu and Rise molecules with the two apatite surfaces. However, the second adsorption energy ($-\varepsilon_2$) is associated to the interactions between the Tilu and Rise molecules of all subsequent layers (i.e., risedronate-risedronate and tiludronate-tiludronate interactions) [20]. It is important to mention that the second adsorption energy ($-\varepsilon_2$) characterizes the interactions of a variable number of layers, which is noted as N_c . The partition function related to D_{sr} receptor sites is written as follows:

$$Z_{gc} = \left[1 + e^{\beta(\varepsilon_1 + \mu)} + e^{\beta(\varepsilon_1 + \varepsilon_2 + 2\mu)} \frac{1 - e^{\beta(\varepsilon_2 + \mu)^{N_c}}}{1 - e^{\beta(\varepsilon_2 + \mu)}}\right]^{D_{sr}} \tag{12}$$

Then, the mathematical expression of the saturated multilayer model is represented by the following equation [20]:

$$Q_a = n_{ms} \cdot D_{sr} \frac{2\left(\frac{C}{C_{hs1}}\right)^{2n_{ms}} + \left(\frac{C}{C_{hs1}}\right)^{n_{ms}} \left(1 - \left(\frac{C}{C_{hs1}}\right)^{2n_{ms}}\right)}{\left(1 - \left(\frac{C}{C_{hs1}}\right)^{n_{ms}}\right) + \left(1 - \left(\frac{C}{C_{hs1}}\right)^{n_{ms}}\right)^2} + \frac{2\left(\frac{C}{C_{hs1}}\right)^{n_{ms}} \left(\frac{C}{C_{hs2}}\right)^{n_{ms}} \left(1 - \left(\frac{C}{C_{hs2}}\right)^{(n_{ms}N_c)}\right)}{\left(1 - \left(\frac{C}{C_{hs2}}\right)^{n_{ms}}\right)} + \frac{\left(\frac{C}{C_{hs1}}\right)^{n_{ms}} \left(\frac{C}{C_{hs2}}\right)^{n_{ms}} \left(\frac{C}{C_{hs2}}\right)^{(n_{ms}N_c)} N_c \left(\frac{C}{C_{hs1}}\right)^{n_{ms}} \left(\frac{C}{C_{hs2}}\right)^{(2n_{ms})} \left(1 - \left(\frac{C}{C_{hs2}}\right)^{(n_{ms}N_c)}\right)}{\left(1 - \left(\frac{C}{C_{hs2}}\right)^{n_{ms}}\right) + \left(1 - \left(\frac{C}{C_{hs2}}\right)^{n_{ms}}\right)^2} + \frac{\left(1 - \left(\frac{C}{C_{hs1}}\right)^{2n_{ms}}\right) \left(\frac{C}{C_{hs1}}\right)^{n_{ms}} \left(\frac{C}{C_{hs2}}\right)^{n_{ms}} \left(1 - \left(\frac{C}{C_{hs2}}\right)^{(n_{ms}N_c)}\right)}{\left(1 - \left(\frac{C}{C_{hs1}}\right)^{n_{ms}}\right) + \left(1 - \left(\frac{C}{C_{hs2}}\right)^{n_{ms}}\right)} \tag{13}$$

where C_{hs1} and C_{hs2} are the concentration at half-saturation of the first and second adsorbed layers involved in the adsorption of Tilu and Rise on two employed adsorbents (HA and NCA).

The schematic illustration of the BP molecules adsorbed on a solid is depicted in Figs. 1, 2 and 3 according to the monolayer model with single energy, the double layer model with two energies and the multilayer model with saturation, respectively.

4. Results and discussion

4.1. Non-linear fitting with isotherm models

Fig. 4 depicts the experimental adsorption data for Risedronate (Rise) and Tiludronate (Tilu) on well-crystallized hydroxyapatite (HA) and nanocrystalline apatites (NCA) at the fixed temperature $T = 310$ K, while Fig. 5 illustrates the data for Rise on HA over the range 6.6–9.5 of pH at $T = 298$ K. Adsorption isotherms were examined by non-linear curve fitting analysis, using ORIGIN software (OriginLab Corporation) to adjust the three aforementioned adsorption models. The best adjusted adsorption isotherm was identified using three parameters: the determination coefficient R^2 , the analysis of the residual root mean square error (RMSE), also called the estimated standard error of the regression, and the akaike information criterion (AIC). These are the most frequently utilized parameters to identify the optimum isotherm model. The determination coefficient R^2 is given by [21]:

$$R^2 = 1 - \left[\left(\frac{\sum_i^m (Q_{i, \text{exp}} - \bar{Q}_{i, \text{exp}})^2 - \sum_i^m (Q_{i, \text{exp}} - Q_{i, \text{model}})^2}{\sum_i^m (Q_{i, \text{exp}} - \bar{Q}_{i, \text{exp}})^2} \right) \times \frac{[n_p - 1]}{[n_p - p]} \right] \tag{14}$$

where, $Q_{i, \text{model}}$ is the i th value of Q predicted by the fitted model, $Q_{i, \text{exp}}$ is the i th value of Q measured experimentally, Q_{exp} is the average value of Q measured experimentally, n_p is the number of performed experiments and p is the number of parameters of the adjusted model.

For a number p of adjustable parameters, the estimated standard error is given by [22]:

$$RMSE = \sqrt{\frac{RSS}{m' - p}} \tag{15}$$

where RSS is the residual sum of squares expressed as $RSS = \sum_{j=1}^{m'} (Q_{j, \text{cal}} - Q_{j, \text{exp}})^2$, $Q_{j, \text{cal}}$ and $Q_{j, \text{exp}}$ are the calculated and experimental values of the adsorbed amount, respectively, and m' is the number of experimental data.



Fig. 1. Schematic illustration of the distribution of the molecules adsorbed on a solid according to the monolayer model with single energy.

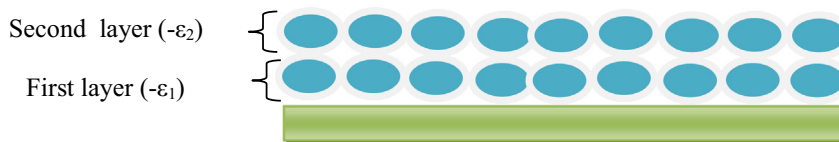


Fig. 2. Schematic illustration of the distribution of the molecules adsorbed on a solid according to the double layer model with two energies.

Then, the estimator of the relative quality of statistical physics models for a given data set AIC is defined as [22]:

$$AIC = k \ln \left(\frac{RSS}{k} \right) + 2p \quad (16)$$

where k represents the number of experimental data points of the adsorption isotherm.

The estimated values of R^2 , RMSE and AIC coefficients are depicted in Table 2. Referring to these values, it is noted that the double layer model with two energies (M2) has the highest R^2 values and the lowest RMSE and AIC values compared to the other models. In addition, there is a slight variation of these coefficients between the three models. This means that our selection must also take into account the physical justification in the chosen model. Moreover the parameter values of the adjusted monolayer model were not consistent with the experimental results. These parameters values have not physical significations and, therefore, the single layer model was discarded for the adsorption data modeling. Regarding the multilayer model, the results of isotherms fitting indicate that the total number of adsorbed layers ($1 + N_c$) varies from 1.79 to 2.23. This indication demonstrates that the adsorption of BPs drugs on the two tested adsorbents is created by a fixed number of layers, which is equal to 2. Finally, the double layer model has acceptable fitting coefficients and reasonable physical parameters. Therefore, it is selected to provide a valuable analysis of the BPs adsorption mechanism. Its fitting parameters are illustrated in Table 3.

4.2. Interpretation of the effect of pH on the adsorption process via the analysis of the model fitting parameters

The purpose of this section is to interpret and fully understand the adsorption mechanism through the analysis of the physicochemical parameters included in the double layer model with two energies. These parameters are analyzed while varying several external chemical factors (temperature and pH).

The different parameters of the chosen model are classified into two types: steric parameters, such as n_{ms} , D_{st} and Q_{asat} , and energetic parameters, such as ΔE_1 and ΔE_2 .

4.2.1. Analysis of the parameter n_{ms}

The parameter n_{ms} expresses the number of Rise and Tilu molecules aggregated on one receptor site. It plays an important role in retrieving further useful indications about the adsorption mechanism. This steric coefficient can provide valuable information on the behavior of the drug molecules after adsorption. In particular, it can determine the degree of aggregation of the drug molecules and their adsorption positions on the apatite surface of both adsorbents (NCA and HA). The estimated values of this parameter (Table 3) indicate that the number of drug molecules differs for the Rise-NCA and Rise-HA systems compared to the Tilu-HA system. For instance, at 310 K and 7.4 pH, the values of n_{ms} are 0.48, 1.12 and 1.24 for Tilu-HA, Rise-NCA and Rise-HA, respectively. Based on this result, it is noted that the estimated values of n_{ms} for the adsorption of Rise on NCA and HA are higher than that obtained with the adsorption of Tilu on HA at a fixed temperature: $n_{ms}(\text{Rise/HA}) > n_{ms}(\text{Rise/NCA}) > n_{ms}(\text{Tilu/HA})$. This trend is probably due to the difference between the two chemical structures of drugs. It is clear that this difference could be related to the presence of the nitrogen atom within the heterocyclic ring on the Rise molecule. This could facilitate the molecule coordination via specific interactions with the main functional groups responsible for the adsorption, and hence seems to explain why the number of Rise molecules adsorbed per site is higher than that found in Tilu drug [3]. As stated, the parameter n_{ms} is also useful to illustrate the behavior of both drugs after adsorption, mainly their adsorption orientations on the apatite adsorbent surface. Since the values of n_{ms} for the Rise drug adsorption were superior to unity and $1 \leq n_{ms} \leq 2$, it can be concluded that each receptor site accepted one or two Rise molecules. Therefore, we assume that the Rise drug was linked to (with) a non-parallel position on the NCA and HA surface. This theoretical result also indicated that the Rise drug only forms a monomer ($n \approx 1$) and a dimer ($n \approx 2$) (see Fig. 6). The aggregation of multiple Rise molecules is favored, indicating that the interaction between the Rise molecules is greater than that between the Rise molecule and the receptor site of apatite. Contrary to this result, the value of n_{ms} for the Tilu adsorption is < 1 . This result suggests that the Tilu drug molecules interacted with two ($(1/0.48) \approx 2$) binding sites and, therefore, the sorption position of this drug was parallel. This parallel position means that the interaction between the Tilu molecules is less than that between the Tilu molecule

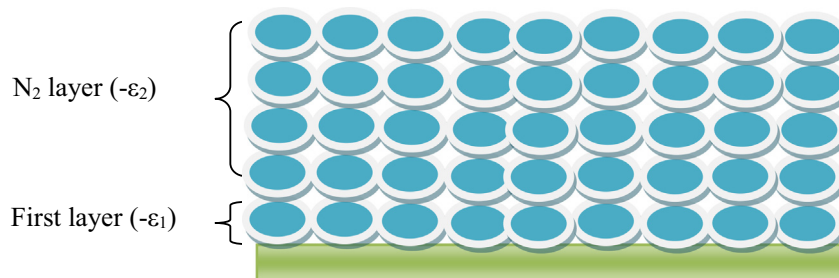


Fig. 3. Schematic illustration of the distribution of the molecules adsorbed on a solid according to the multilayer model with saturation.

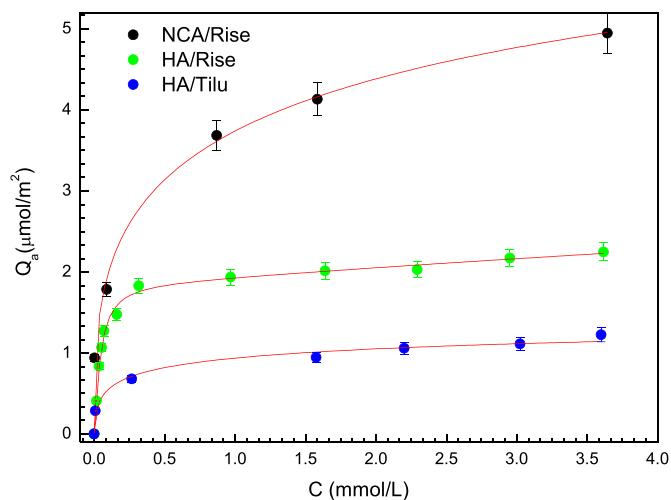


Fig. 4. Adsorption isotherms of tiludronate (Tilu) and risedronate (Rise) at 310 K and pH 7.4 on HA and NCA and fitting by double layer statistical physics model (M2).

and the receptor site of apatite. Therefore, the main functional groups may only select a fraction of Tilu molecules leading to an absence of the adsorbate aggregation in the aqueous solution. The effect of pH on n_{ms} at room temperature is depicted in Table 3 and Fig. 7. It is clear that the variation of pH had a slight effect on the adsorbate orientation of the Rise drug on HA. The number of Rise molecules per site increases with pH. The increase of pH means a decrease in the concentration of the H^+ ions. So the increase of H^+ (i.e. decrease of pH) decreases n_{ms} . The existence of H^+ ions decreases the interaction between the Rise molecules and increases the interaction between the Rise molecules and the receptor sites of the HA apatite as we will see in the next paragraph. So the presence of H^+ does not favor the aggregation of Rise drug molecules. Therefore, n_{ms} increases with pH. The values of n_{ms} for Rise-HA decrease as a function of temperature. This behavior could be explained by thermal agitation that causes thermal collisions between the drug molecules. These collisions lead to an uncoupling of Rise molecules from the receptor site, then to a decrease of the number of Rise molecules captured per binding site.

4.2.2. Analysis of the parameter D_{sr}

On the other hand, the parameter D_{sr} is defined as the density of receptor sites, i.e. the number of the occupied receptor sites per surface

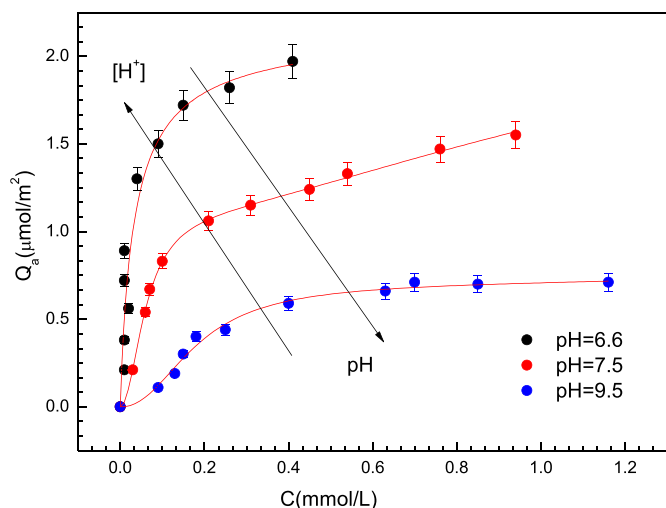


Fig. 5. Adsorption isotherms of risedronate (Rise) on HA at 298 K for different pH values and fitting by double layer statistical physics model (M2).

Table 2 Values of coefficient of determination R^2 , AIC and RMSE of each model.

Adsorbent	pH	T(K)	Model		
			Model 3	Model 2	Model 1
			R^2		
RISE-NCA	7.4	310	0.9865	0.9903	0.9768
RISE-HA	7.4	310	0.9811	0.9951	0.9727
TILU-HA	7.4	310	0.9825	0.9981	0.9779
RISE-HA	6.6	298	0.9830	0.9991	0.9781
	7.4	298	0.9832	0.9997	0.9768
	9.5	298	0.9886	0.9954	0.9736
			RMSE		
RISE-NCA	7.4	310	0.032	0.001	0.401
RISE-HA	7.4	310	0.082	0.002	0.183
TILU-HA	7.4	310	0.073	0.008	0.152
RISE-HA	6.6	298	0.041	0.005	0.115
	7.4	298	0.023	0.009	0.157
	9.5	298	0.003	0.003	0.353
			AIC		
RISE-NCA	7.4	310	4.53	2.56	13.15
RISE-HA	7.4	310	6.08	1.87	14.28
TILU-HA	7.4	310	5.37	1.45	12.35
RISE-HA	6.6	298	5.04	1.12	12.11
	7.4	298	4.82	1.32	13.15
	9.5	298	4.22	2.07	14.13

unit. The calculated values of this parameter are illustrated in Table 3 and Fig. 7. We can note that the density of the receptor site decreases with the increase in pH from 6.6 to 9.5. This means that D_{sr} decreases when H^+ concentration decreases. As we saw in the previous paragraph, the presence of H^+ inhibits the aggregation phenomenon of Rise molecules. Thus, at high pH, $[H^+]$ is low, the aggregation phenomenon is reinforced and the size of aggregation increases. This size could inhibit the reachability of the other adsorption sites by a steric effect, causing D_{sr} to be low. Moreover this parameter evolves in an opposite manner with respect to n_{ms} . The aggregation phenomenon is inhibited. All the molecules of aggregates are dispersed horizontally on the other sites. By an energetic effect, the affinity of the Rise molecules is decreased. However the affinity between the Rise molecules and the receptor sites is increased. This causes an increase of D_{sr} and consequently an increase of the adsorption quantity as shown in Fig. 5 for different values of pH. Both the steric and energetic effects contribute similarly.

4.2.3. Analysis of the parameter Q_{asat}

The uptake capacity at saturation obtained via the analytical double layer adsorption model ($Q_{asat} = 2 \cdot n_{ms} \cdot D_{sr}$) is clearly a useful parameter that characterizes the adsorption process. Indeed, this parameter reflects the total number of adsorbed Rise molecules. $Q_{asat} = 2 \cdot n_{ms} \cdot D_{sr}$ is the total number of adsorbed molecules per layer. The scalar 2 represents the two layers of the chosen model. Q_{asat} indicates the adsorbent performance or the affinity with the adsorbates which can be affected by some external chemical factors (e.g. temperature and pH). The calculated values of this parameter for a fixed pH 7.4 and a fixed temperature (310 K) are depicted in Table 3. The results show that

Table 3 Values of the different adjusted parameters according to double layer model with two energies (M2).

Adsorbent	pH	T(K)	Parameters				
			n_{ms}	D_{sr} ($\mu\text{mol}/\text{m}^2$)	Q_{asat} ($\mu\text{mol}/\text{m}^2$)	ΔE_1 (kJ/mol)	ΔE_2 (kJ/mol)
RISE-NCA	7.4	310	1.12	2.45	5.10	15.77	9.20
RISE-HA	7.4	310	1.24	1.50	3.72	18.64	11.43
TILU-HA	7.4	310	0.48	1.69	1.62	12.36	7.84
RISE-HA	6.6	298	1.15	0.92	2.11	19.52	14.08
	7.4	298	1.75	0.42	1.70	17.04	13.41
	9.5	298	1.89	0.22	0.96	14.32	9.97

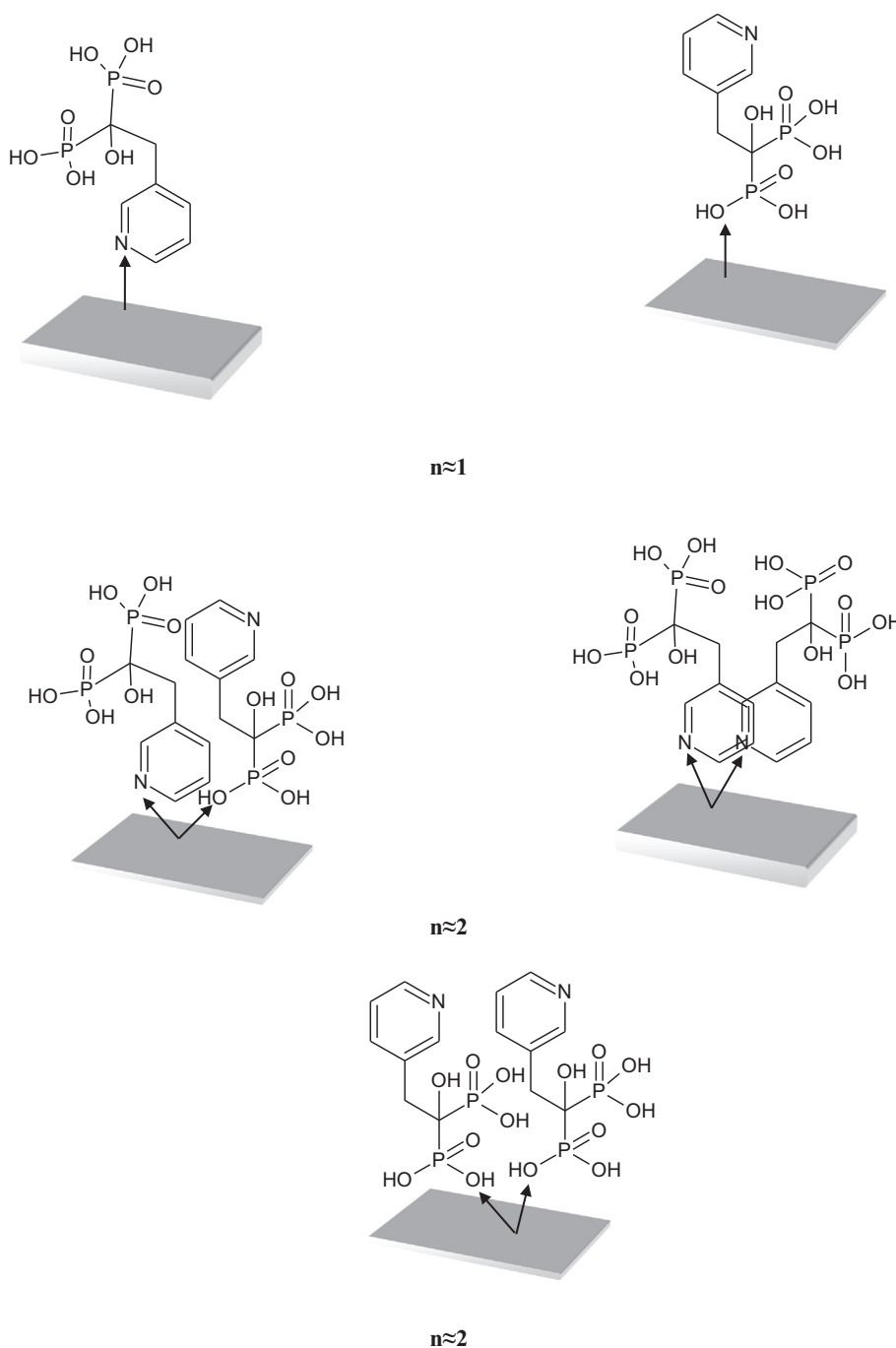


Fig. 6. Schematic illustration of the possible aggregation of Rise molecule on apatite surface.

this parameter varies as follows: $Q_{\text{asat}}(\text{Rise/NCA}) > Q_{\text{asat}}(\text{Rise/HA}) > Q_{\text{asat}}(\text{Tilu/HA})$. This sequence demonstrates that the quantity adsorbed at saturation on the HA specimen appears lower for Tilu than Rise. This is mainly explained by the chemical structure of the bisphosphonates which can affect their adsorption capacities for HA and NCA. The risedronate molecule contains a nitrogen atom within the functional groups of the heterocyclic ring. This could facilitate and improve the molecule ability to bind via specific interactions with the apatite surface, and enhance its uptake capacity [3]. Moreover, we can also note that the amount of Rise adsorbed at saturation on NCA appears higher than that found on HA. This result suggests that the uptake capacity at saturation is strongly influenced not only by the chemical characteristics of the drug molecule, but also by the chemical and structural properties of the apatite compounds. NCA exhibits the highest

adsorption capacity of Rise molecules compared to HA adsorbent indicating its better affinity for this drug. This result is in agreement with several published studies [23–25]. This could also be attributed to the hydrated layer rich in chemical species presented on the surface of NCA which is responsible for a high adsorption capacity [26].

Recall that this parameter depends mainly on various factors including temperature and pH. In particular, the influence of temperature, at pH 7.4 for example, indicates a higher adsorption capacity of Rise on HA at physiological temperatures compared with room temperature. However in terms of comparison with the case of the variation of pH at 298 K, Table 3 and Fig. 7 show that the amount of Rise adsorbed at saturation decreases as the pH rises. As it can be seen, the loaded amount at pH 6.6 is about three times higher than that obtained at pH 9.5. This is probably caused by the weakening of electrostatic force of attraction

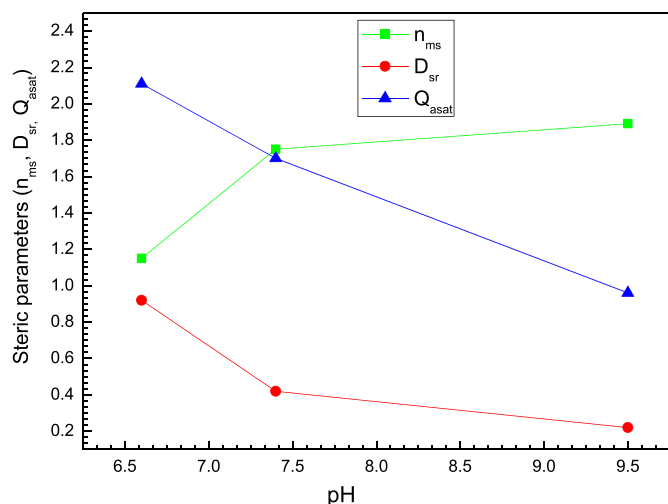


Fig. 7. Effect of pH on the number of Rise molecules, the density of receptor sites and Rise adsorption capacity at saturation onto HA adsorbent.

between the adsorbate and adsorbent which are oppositely charged and led to the decrease of the sorption capacity [27]. More precisely, with the increase of pH, the H^+ ion concentration decreases and hence the positively charged sites of the adsorbent get decreased and the surface of the adsorbent became negatively charged. Consequently, the adsorption of Rise drug by the system is no longer promoted and electrostatic repulsion occurs [27]. At high pH, an effective competition occurs between OH^- ions and Rise drug molecules, and causes a decrease in sorption of the drug from aqueous solutions. Moreover, the pH variation affects the adsorption process by the dissociation of functional groups on the HA adsorbent surface which tends to shift in the equilibrium of the adsorption phenomenon. As mentioned above, the capacity is $Q_{asat} = 2 \cdot n_{ms} \cdot D_{sr}$. It is the result of two different contributions: that of n_{ms} which expresses the aggregation phenomenon evolution and that of D_{sr} evolution. We have already studied the two behaviors of n_{ms} and D_{sr} and their interpretations. Although the two evolutions of n_{ms} and D_{sr} are antagonistic, never the less the evolution of D_{sr} prevails over that of n_{ms} . This is proved by numerical calculation and verified in Fig. 5. It is worth noting that the increase of the uptake of Rise is essentially due firstly to a steric effect caused by the H^+ ions which inhibit the aggregation phenomenon resulted in an increase of D_{sr} , and secondly to an energetic effect favoring an affinity between Rise molecules and receptor sites. This affinity is expressed by the adsorption energy as we will see in the next paragraph.

4.2.4. Analysis of the energetic parameters of the adsorption surface

The adsorption energy is an important parameter which is required to investigate the adsorption process and to retrieve information about adsorbate-adsorbent interactions. From the two concentrations at half saturation C_{hs1} and C_{hs2} , it is possible to estimate the two adsorption energies (ΔE_1) and (ΔE_2) using an analytical expression deduced from the statistical physics treatment. Specifically, ΔE_1 is related to the interactions between the drug molecules and the apatite surface (Rise-NCA/HA, and Tilu-HA) on the first layer, while ΔE_2 characterizes the interactions between the drug molecules themselves (Rise-Rise and Tilu-Tilu) on the second layer. The expressions of these energies are given by:

$$\Delta E_1 = RT \ln \frac{C_s}{C_{hs1}} \quad (17)$$

$$\Delta E_2 = RT \ln \frac{C_s}{C_{hs2}} \quad (18)$$

where C_s is the solubility of the adsorbate, R is the ideal gas constant and T is the absolute temperature. To simplify the analysis, the molecule

solubility of the two drugs was assumed to be constant at the two considered temperatures. The estimated values of the adsorption energies are summarized in Table 3. First, all the values of the adsorption energies obtained by the fitting process are lower than 20 kJ/mol. This indicates that the adsorption process is characterized by physical interactions which may be in the form of hydrogen bonding or Van der Waals interactions. The hydrogen bonding usually represents values lower than 30 kJ/mol and the Van der Waals forces are generally of the order of 10 kJ/mol [28,29]. As expected, the first energy is found to be higher than the second one, due to the weaker interactions between Rise-Rise and Tilu-Tilu. Finally, by plotting ΔE_1 and ΔE_2 against pH for the Rise molecules in Fig. 8, we can notice that the two energies decrease with the increasing pH or increase with the increased concentration of H^+ ions. This confirms what we have advanced in the previous paragraph concerning the interpretation of the parameters n_{ms} and D_{sr} against pH. We show here in Fig. 8 that the presence of H^+ ions (inversely to pH) increases the two adsorption energies ΔE_1 and ΔE_2 , resulting in the inhibition by H^+ of the aggregation of Rise molecules.

4.3. Thermodynamic studies

Thermodynamic parameters like internal energy, free enthalpy and entropy were calculated with our advanced double layer model with two energies in order to evaluate the feasibility and nature of the adsorption reaction. These thermodynamic functions are investigated in the following part.

4.3.1. Internal energy

The internal energy is given by [30]:

$$E_{int} = -\frac{\partial \ln Z_{gc}}{\partial \beta} + \frac{\mu}{\beta} \left(\frac{\partial \ln Z_{gc}}{\partial \mu} \right) \quad (19)$$

Finally, the expression of the internal energy is given by:

$$\frac{E_{int}}{K_B T} = D_{sr} \left[\ln \left(\frac{C}{Z_v} \right) \cdot \left(\frac{\left(\frac{C}{C_{hs1}} \right)^{n_{ms}} + \left(\frac{C}{C_{hs2}} \right)^{2n_{ms}}}{1 + \left(\frac{C}{C_{hs1}} \right)^{n_{ms}} + \left(\frac{C}{C_{hs2}} \right)^{2n_{ms}}} \right) - \frac{\left(\frac{C}{C_{hs1}} \right)^{n_{ms}} \cdot \ln \left(\frac{C}{C_{hs1}} \right)^{n_{ms}} + \left(\frac{C}{C_{hs2}} \right)^{2n_{ms}} \cdot \ln \left(\frac{C}{C_{hs1}} \right)^{2n_{ms}}}{1 + \left(\frac{C}{C_{hs1}} \right)^{n_{ms}} + \left(\frac{C}{C_{hs2}} \right)^{2n_{ms}}} \right] \quad (20)$$

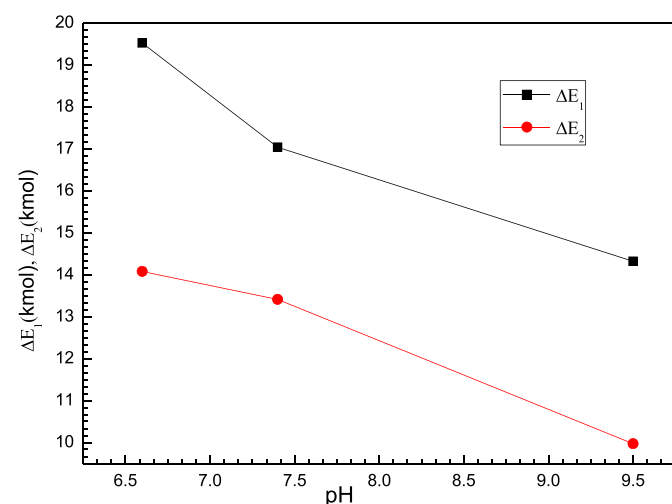


Fig. 8. Effect of pH on the Rise adsorption energy (ΔE_1 and ΔE_2) of HA.

where Z_v is the translation partition function per unit of volume of the adsorbate molecule.

The variation of the internal energy is illustrated in Fig. 9. According to this figure, we can note that this parameter is negative and releases energy. This confirms that the three systems (i.e. Rise-NCA, Rise-HA and Tilu-HA) evolve spontaneously.

4.3.2. Gibbs energy

The free enthalpy is given as follows [30]:

$$G = \mu Q_a \quad (21)$$

In addition, by incorporating Eq. (11) into Eq. (21), the free enthalpy can be written as follows:

$$\frac{G}{K_B T} = \ln \left(\frac{C}{Z_v} \right) \cdot \left(n_{ms} \cdot D_{sr} \cdot \frac{\left(\frac{C}{C_{hs1}} \right)^{n_{ms}} + 2 \left(\frac{C}{C_{hs2}} \right)^{2n_{ms}}}{1 + \left(\frac{C}{C_{hs1}} \right)^{n_{ms}} + \left(\frac{C}{C_{hs2}} \right)^{2n_{ms}}} \right) \quad (22)$$

Fig. 10 shows the free enthalpy as a function of the equilibrium concentration for the adsorption of two drugs on apatite substrates. The values of the free enthalpy of all the systems are negative confirming that the drugs adsorption on NCA and HA is spontaneous.

4.3.3. Entropy

The absorption entropy is related to the grand potential by the following equations [30]:

$$J = -k_B T \ln Z_{gc} \quad (23)$$

$$J = -\frac{\partial \ln Z_{gc}}{\partial \beta} - T S_a \quad (24)$$

From Eqs. (23) and (24), the expression of the entropy can be derived as follows:

$$\frac{S_a}{k_B} = -\beta \frac{\partial \ln Z_{gc}}{\partial \beta} + \ln Z_{gc} \quad (25)$$

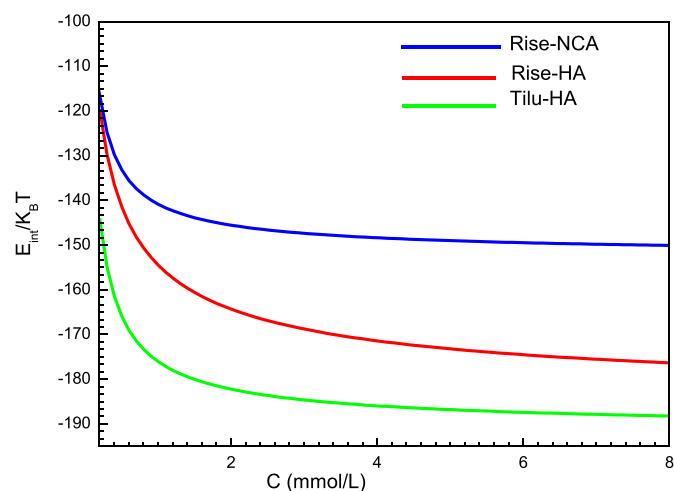


Fig. 9. Variation of internal energy versus concentration for the three studied systems at 310 K and pH 7.4.

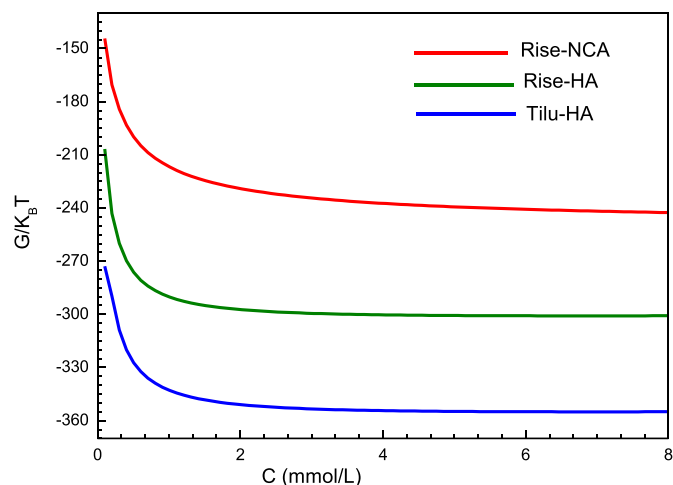


Fig. 10. Variation of the free enthalpy versus concentration for the three studied systems at 310 K and pH 7.4.

According to the double layer model with two energies, the entropy is expressed as follows:

$$\frac{S_a}{k_B} = D_{sr} \left[\ln \left(1 + \left(\frac{C}{C_{hs1}} \right)^{n_{ms}} + \left(\frac{C}{C_{hs2}} \right)^{2n_{ms}} \right) - \frac{\left(\frac{C}{C_{hs1}} \right)^{n_{ms}} \cdot \ln \left(\frac{C}{C_{hs1}} \right)^{n_{ms}} + \left(\frac{C}{C_{hs2}} \right)^{2n_{ms}} \cdot \ln \left(\frac{C}{C_{hs1}} \right)^{2n_{ms}}}{1 + \left(\frac{C}{C_{hs1}} \right)^{n_{ms}} + \left(\frac{C}{C_{hs2}} \right)^{2n_{ms}}} \right] \quad (26)$$

Fig. 11 illustrates the entropy variation as a function of concentration for the adsorption of two bisphosphonates (Rise and Tilu) on the tested adsorbents. For the three employed systems, the entropy has a similar shape. It is also shown that the variation of entropy indicates two peaks associated respectively to the first and the second concentrations (C_{hs1}) and (C_{hs2}). The shape of the entropy at the two peaks follows two different behaviors before and after the half-saturation concentration. The entropy S_a starts from a null value at the beginning of the adsorption and then reaches a maximum in the proximity of the first half-saturation, for $C = C_{hs1}$. This indicates that the disorder is at the maximum when half of the receptor sites of the first layer are occupied. Then, the entropy decreases when all the binding sites of the first layer are fully occupied. Indeed, for a low concentration ($C < C_{hs1}$), the

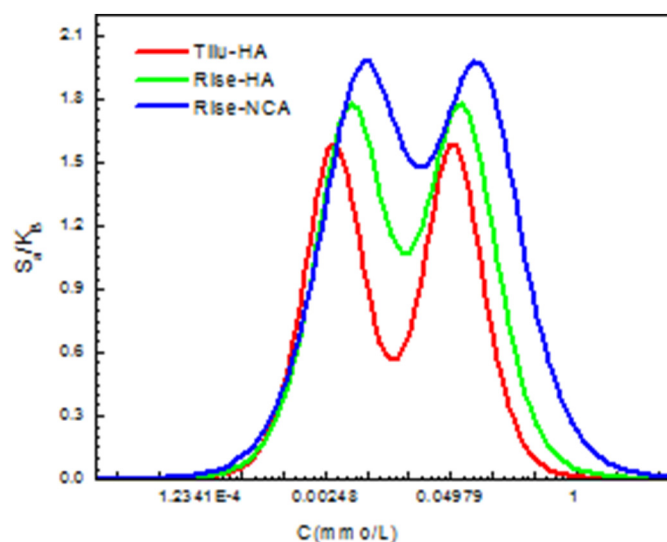


Fig. 11. Variation of the entropy versus concentration for the three studied systems at 310 K and pH 7.4.

molecule has many possibilities to find a vacant site and, consequently, the disorder rises at the surface with the uptake capacity. After the first half-saturation, the number of empty sites in the 1st sorbed layer diminishes and the number of available sites becomes limited. Therefore, the entropy decreases since the possibilities of finding a free site of the first type diminish more and more when the saturation of the first adsorbed layer is almost attained. The detected minimum value of the entropy does not reach zero, because the second-type site begins to fill before the complete saturation of the first one. The same entropy behavior can be observed since the first layer is employed as adsorbent sites for the second layer. Finally, the entropy can reach zero when the saturation is attained.

4.3.4. The comparison between the three adsorption systems

From Figs. 9, 10 and 11, we can obviously notice that, at a fixed pH = 7.4, the order of classification of the energetic potentials is the same, and potential Tiliu-HA⁻ potential Rise-HA⁻ potential Rise-NCA. This order is proportional to the adsorbed quantity Q_a . So this adsorption process varies in the same way as the corresponding energetic potential. However, the entropy whose energetic potential is TS, and which expresses a thermal agitation, varies in an opposite way to the energetic potentials, like the adsorbed quantity Q_a . This highlights the importance of the configurational entropy which increases the thermal disorder but slows down the adsorption process despite the increase of the adsorption configurations. Therefore, the best adsorption system is the one with low entropy.

5. Conclusion

The present study reported a new theoretical formalism to investigate the adsorption of two bisphosphonates (risedronate and tiludronate) on two apatite supports, namely a well-crystallized hydroxyapatite (HA) and nanocrystalline apatites (NCA). The double layer model with two energies developed using the grand canonical partition function provided the perfect fit of the experimental data, among the tested models. The bisphosphonate (BP) adsorption isotherms on the two apatite substrates were analyzed and interpreted in the light of this model and of its parameters, related to defined physical meanings. The results showed that two different adsorption positions of the Rise and Tiliu molecules, parallel and non-parallel to the surface of HA and NCA, could be observed depending on the adsorbents properties. The uptake capacity at saturation of Rise on NCA specimen seems higher than that obtained for Rise on HA and Tiliu on HA. This suggests that both the chemical characteristics of the drug molecules and the chemical and structural properties of the apatite substrates strongly affect the capacity of adsorption. The influence of pH on the evolution of the steric and energetic parameters has been investigated. The number of Rise molecules per HA adsorbent site increases in proportion to pH. This increase of the n_{ms} values was associated with a reduction in the adsorption capacity and in the densities of the receptor sites. Hence, an acidic condition caused by H⁺ ions is more favorable for the Rise adsorption process. The estimated values of the adsorption energies were lower than 20 kJ/mol and confirmed the occurrence of a physisorption process. The thermodynamic study confirmed the feasibility and spontaneous nature of the adsorption of these drugs on tested adsorbents.

Credit author statement

Aljawhara H. Almuqrin: Writing- original draft; Conceptualization; Funding acquisition; Project administration; Resources. **Sarra Wjihi:** Writing - review & editing; Investigation; Validation; Data curation. **Fatma Aouaini:** Software; Methodology; Formal analysis. **Abdelmottaleb Ben Lamine:** Supervision; Visualization.

Declaration of competing interest

This submission has not been published previously and not under consideration for publication elsewhere. If it will be published, it will not be published elsewhere in the same form, in English or in any other language, including electronically without the written consent of the copyright-holder.

Acknowledgments

The authors would like to thank the Center for Promising Research in Social Research and Women's Studies Deanship of Scientific Research, at Princess Nourah Bint Abdulrahman University for funding this Project in 2020.

References

- [1] G.A. Rodan, H.A. Fleisch, Bisphosphonates: mechanisms of action, *J. Clin. Invest.* 97 (12) (1996) 2692.
- [2] R.G.G. Russell, et al., Mechanisms of action of bisphosphonates: similarities and differences and their potential influence on clinical efficacy, *Osteoporos. Int.* 19 (6) (2008) 733–759.
- [3] G.H. Nancollas, et al., Novel insights into actions of bisphosphonates on bone: differences in interactions with hydroxyapatite, *Bone* 38 (5) (2006) 617–627.
- [4] S.N. Elliott, et al., Alendronate induces gastric injury and delays ulcer healing in rodents, *Life Sci.* 62 (1) (1997) 77–91.
- [5] N. Demerjian, G. Bolla, A. Spreux, Severe oral ulcerations induced by alendronate, *Clin Rheumatol* 18 (4) (1999) 349–350.
- [6] M. Kos, K. Luczak, Bisphosphonates promote jaw osteonecrosis through facilitating bacterial colonisation, *Biosci Hypotheses* 2 (1) (2009) 34–36.
- [7] J. Monkkonen, J. Simila, M.J. Rogers, Effects of tiludronate and ibandronate on the secretion of proinflammatory cytokines and nitric oxide from macrophages in vitro, *Life Sci.* 62 (8) (1998) PL95–PL102.
- [8] S. Mukherjee, Y. Song, E. Oldfield, *J. Am. Chem. Soc.* 130 (2008) 1264.
- [9] A. Juillard, G. Falgayrac, B. Cortet, M.-H. Vieillard, N. Azaroual, J.-C. Hornez, G. Penel, *Bone* 47 (2010) 895.
- [10] S. Josse, C. Fauchoux, A. Soueidan, G. Grimandi, D. Massiot, B. Alonso, P. Janvier, S. Laib, P. Pilet, O. Gauthier, G. Daculsi, J. Guicheux, B. Bujoli, J.-M. Bouler, *Biomaterials* 26 (2005) 2073.
- [11] I. Cukrowski, L. Popovic, W. Barnard, S.O. Paul, P.H. van Rooyen, D.C. Liles, *Bone* 41 (2007) 668.
- [12] F. Errassifi, et al., Adsorption on apatitic calcium phosphates: application to drug delivery, in: *A.C. Soc. (Ed.), 8th Pacific Rim Conference on Ceramic and Glass Technology 2010*, pp. 159–174, Vancouver.
- [13] P. Pascaud, et al., Interaction between a bisphosphonate, tiludronate, and biomimetic nanocrystalline apatites, *Langmuir* 29 (2013) 2224–2232.
- [14] B. Palazzo, et al., Biomimetic hydroxyapatite-drug nanocrystals as potential bone substitutes with antitumor drug delivery properties, *AdvFunc Mater* 17 (13) (2007) 2180–2188.
- [15] F.H. Browning, H.S. Fogler, *Langmuir* 12 (1996) 5231.
- [16] A.T. Kan, J.E. Oddo, M.B. Tomson, *Langmuir* 10 (1994) 1450.
- [17] Patricia Pascaud, Farid Errassifi, Fabien Brouillet, Stéphanie Sarda, Allal Barroug, et al., Adsorption on apatitic calcium phosphates for drug delivery: interaction with bisphosphonate molecules, *Journal of Materials Science: Materials in Medicine*, Springer Verlag 25 (10) (2014) 2373–2381.
- [18] M. Khalifaoui, S. Knani, M.A. Hachicha, A. Ben Lamine, New theoretical expressions for the five adsorption type isotherms classified by BET based on statistical physics treatment, *J. Colloid Interf. Sci.* 263 (2003) 350–356.
- [19] M. Khalifaoui, M.H.V. Baouab, R. Gauthier, A. Ben Lamine, *J. Adsorption Science & Technology* 20 (2002) 17–31.
- [20] S. Wjihi, A. Erto, S. Knani, A.B. Lamine, Investigation of adsorption process of benzene and toluene on activated carbon by means of grand canonical ensemble, *J. Mol. Liq.* 238 (2017) 402–410.
- [21] D.W. Marquardt, *J. Soc. Ind. Appl. Math.* 11 (1963) 431–441.
- [22] D.G. Kinniburgh, J.A. Barker, M.A. Whitfield, Comparison of some simple adsorption isotherms for describing divalent cation adsorption by ferrihydrite, *J. Colloid Interface Sci.* 95 (1983) 370–384.
- [23] A. Juillard, G. Falgayrac, B. Cortet, M.-H. Vieillard, N. Azaroual, J.-C. Hornez, G. Penel, *Bone* 47 (2010) 895.
- [24] S. Josse, C. Fauchoux, A. Soueidan, G. Grimandi, D. Massiot, B. Alonso, P. Janvier, S. Laib, P. Pilet, O. Gauthier, G. Daculsi, J. Guicheux, B. Bujoli, J.-M. Bouler, *Biomaterials* 26 (2005) 2073.
- [25] P. Pascaud, P. Gras, Y. Coppel, C. Rey, S. Sarda, *Langmuir* 29 (2013) 2224–2232.
- [26] D. Eichert, C. Drouet, H. Sfihi, C. Rey, C. Combes, *Biomater. Res. Adv.* 93 (2008).
- [27] S.S. Baral, S.N. Das, P. Rath, *Biochem. Eng. J.* 31 (2006) 216–222.
- [28] M.T. Ward, P.R. Upchurch, Role of the amino group in adsorption mechanisms, *J. Agric. Food Chem.* 13 (1965) 334–338.
- [29] B. von Oepen, W. Kördel, W. Klein, Sorption of nonpolar and polar compounds to soils: processes, measurements and experience with the applicability of the modified OECD-guideline 106, *Chemosphere* 22 (1991) 285–304.
- [30] L. Couture, R. Zitoun, *Physique statistique*, J. Ellipses 375 (1992).